Title
Thermodynamics of Nanobody Binding to Lactose Permease

Journal
BIOCHEMISTRY, 55(42)

ISSN
0006-2960

Authors
Hariharan, P
Andersson, M
Jiang, X
et al.

Publication Date
2016-10-25

DOI
10.1021/acs.biochem.6b00826

Peer reviewed

BIOCHEMISTRY
including biophysical chemistry & molecular biology

Article

pubs.acs.org/biochemistry

Thermodynamics of Nanobody Binding to Lactose Permease

Parameswaran Hariharan,[†] Magnus Andersson,[‡] Xiaoxu Jiang,[§] Els Pardon,[∥,⊥] Jan Steyaert,[∥,⊥] H. Ronald Kaback,[*,§,#,@] and Lan Guan[*,†]

[†]Department of Cell Physiology and Molecular Biophysics, Center for Membrane Protein Research, School of Medicine, Texas Tech University Health Sciences Center, Lubbock, Texas 79430, United States

[‡]Department of Theoretical Physics and Swedish e-Science Research Center, Science for Life Laboratory, KTH Royal Institute of Technology, SE-171 21 Solna, Sweden

[§]Department of Physiology, University of California, Los Angeles, California 90095, United States

[∥]VIB Center for Structural Biology Research, VIB, 1050 Brussel, Belgium

[⊥]Structural Biology Brussels, Vrije Universiteit Brussel, Pleinlaan 2, 1050 Brussel, Belgium

[#]Department of Microbiology, Immunology and Molecular Genetics and [@]Molecular Biology Institute, University of California, Los Angeles, California 90095, United States

Supporting Information

ABSTRACT: Camelid nanobodies (Nbs) raised against the outward-facing conformer of a double-Trp mutant of the lactose permease of *Escherichia coli* (LacY) stabilize the permease in outward-facing conformations. Isothermal titration calorimetry is applied herein to dissect the binding thermodynamics of two Nbs, one that markedly improves access to the sugar-binding site and another that dramatically increases the affinity for galactoside. The findings presented here show that both enthalpy and entropy contribute favorably to binding of the Nbs to wild-type (WT) LacY and that binding of Nb to double-Trp mutant G46W/G262W is driven by a greater enthalpy at an entropic penalty. Thermodynamic analyses support the interpretation that WT LacY is stabilized in outward-facing conformations like the double-Trp mutant with closure of the water-filled cytoplasmic cavity through conformational selection. The LacY conformational transition required for ligand binding is reflected by a favorable entropy increase. Molecular dynamics simulations further suggest that the entropy increase likely stems from release of immobilized water molecules primarily from the cytoplasmic cavity upon closure.

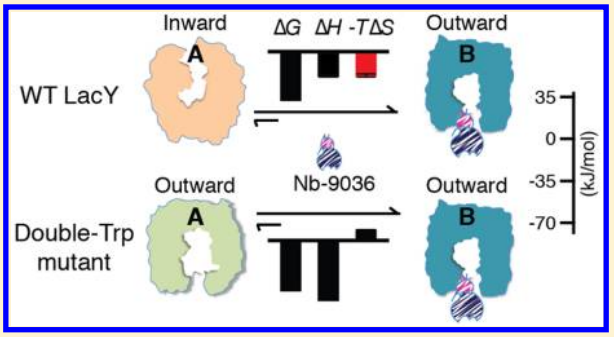

The lactose permease of *Escherichia coli* (LacY) catalyzes galactoside/H^+ symport,[1,2] and crystal structures demonstrate that the N- and C-terminal six-helix bundles surround a central aqueous cavity.[3−8] Most X-ray structures exhibit an inward (cytoplasmic)-facing conformation with a large water-filled cavity[3−6] (Figure 1a). Multiple independent lines of evidence[9−12] indicate that the inward-facing conformation represents the lowest-free energy state of LacY in the absence of bound galactoside in either the membrane-embedded or detergent-solubilized state. A double-Trp mutant (G46W/G262W LacY) shifts the lowest-energy state of LacY into an outward (periplasmic)-facing conformation[13] that crystallizes with an occluded galactoside. While this conformation has a narrow opening to the periplasm, it is tightly sealed to the cytoplasm (Figure 1b).[7,8] In the outward-facing mutant structure, the galactopyranoside moiety is completely liganded by side chains from both the N- and C-terminal bundles.[7,8] Galactoside binding induces a relatively large conformational change that allows LacY to expose sugar- and H^+-binding sites to either side of the membrane via an alternating-access mechanism (reviewed in refs 9 and 14). Evidence indicating that sugar binding involves an induced-fit mechanism, which drives LacY into an occluded intermediate state, has also been presented.[7]

To stabilize WT LacY in an outward-facing conformation for crystallization and structure determination, camelid single-domain nanobodies (Nbs) were raised against a double-Trp mutant.[15] Nine Nbs completely inhibit active lactose transport by right-side-out membrane vesicles containing WT LacY; three inhibit partially, and one does not inhibit significantly.[15] The inhibitory Nbs bind to the periplasmic side of LacY with low nanomolar affinity and stabilize LacY in outward-facing conformations.[15,16] On the basis of stopped-flow fluorimetric measurements,[15] Nb-9036 improves periplasmic access of the WT to *p*-nitrophenyl α-D-galactopyranoside (α-NPG) and also increases the affinity for α-NPG by ~500-fold for the WT and ~80-fold for the mutant by decreasing the dissociation rate. In

Received: August 10, 2016
Revised: September 27, 2016

DOI: 10.1021/acs.biochem.6b00826
Biochemistry XXXX, XXX, XXX−XXX

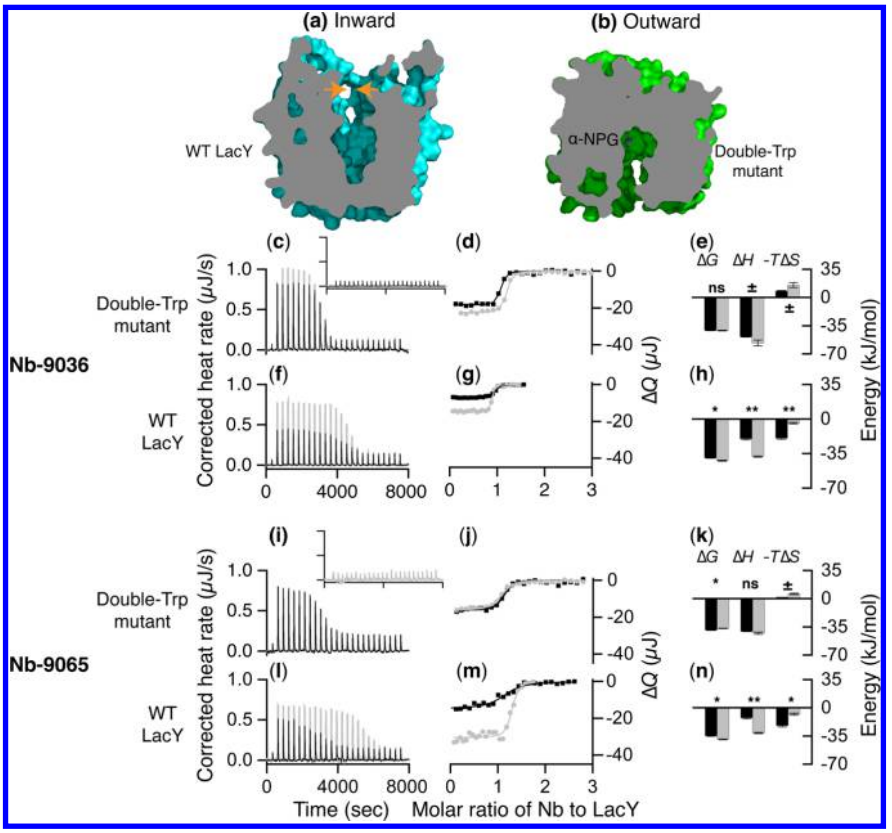

Figure 1. Nb binding to LacY assessed by ITC. Cross section of (a) the inward-facing conformation from the X-ray crystal structure of WT apo LacY (PDB entry 2V8N)[3] or (b) a narrowly outward-facing conformation of G46W/G262W LacY with an occluded α-NPG molecule (PDB entry 4ZYR).[8] The two small orange arrows facing each other in panel a point to the area that closes to form the occluded or outward-facing conformation. (c–n) Nb binding. Titration of G46W/G262W LacY (22 or 25 μM) or WT LacY (40 μM) with Nb-9036 (188 μM) or Nb-9065 (200 μM) in the absence (black) or presence (gray) of melibiose at a saturating concentration of 10 mM was performed with a Nano ITC instrument. (c, f, i, and l) Thermograms were recorded at 25 °C. The inset in panel c is the thermogram from the injection of Nb into buffer without protein. (d, g, j, and m) Accumulated heat change (ΔQ, on the right side) plotted vs the Nb:LacY molar ratio. The data were fitted to a one-site independent binding model, and the results are listed in Table 1. (e, h, k, and n) Comparison of Nb binding energy in the absence (black) and presence (gray) of galactoside. The histograms were generated from data listed in Table 1. An unpaired *t*-test was applied for the statastic anlaysis. When $P > 0.1$, the difference is considered to be not statistically significant (ns). When $P = 0.05–0.1$, the difference is considered to be not quite statistically significant (±). When $P = 0.01–0.05$, the difference is considered to be statistically significant (*). When $P = 0.001–0.01$, the difference is considered to be very statistically significant (**).

contrast, Nb-9065 exhibits little effect on the sugar binding kinetics with the mutant but dramatically improves periplasmic access of α-NPG to the sugar-binding site of the WT to a level similar to that of the outward-facing mutant. Thus, Nb-9065 likely stabilizes the WT in a conformation similar to that of the mutant, and either Nb stabilizes the WT LacY in outward-facing conformations similar to that of the Nb-bound mutant.[15]

Recently, isothermal titration calorimetry (ITC) was utilized to study the thermodynamics of ligand binding with membrane transport proteins.[17–21] The thermodynamics of binding of the cytosolic phosphotransferase protein IIA^{Glc} to the cytoplasmic face of LacY[18] or melibiose permease (MelB),[19] a galactoside/Na^+ symporter,[22–24] have been determined. Although similar binding affinities are observed for the two permeases, thermodynamic features of the binding differ. With *Salmonella typhimurium* melibiose permease ($MelB_{St}$), which crystallizes in an outward-facing conformation,[25] IIA^{Glc} binding is exothermic and driven by enthalpy with entropic compensation.[19] In contrast, with LacY, which favors an inward-facing conformation, binding is endothermic and driven primarily by entropy at the cost of enthalpy.[18] Entropy-driven binding has often been interpreted as a hydrophobic effect caused by release of low-entropy immobilized water molecules from hydrophobic interactions between a ligand and the binding surface.[26–28] However, it has been suggested that large global conformational transitions in LacY and favorable solvation entropy make the primary contribution to the increase in entropy favored by IIA^{Glc} binding.[18] To examine further the correlation between entropy and conformational changes, the thermodynamics of binding of Nb-9036 or Nb-9065 to LacY or the double-Trp mutant, as well as the interplay with sugar and/or IIA^{Glc}, are determined here. The data support the conclusion that conformational selection is involved in binding of Nb to WT LacY, which is promoted by galactoside binding. Furthermore, the conformational transition of WT LacY required for ligand binding—whether the ligand is Nb, a galactoside, or IIA^{Glc}—is reflected by a favorable entropy increase. Molecular dynamics (MD) simulations suggest that the inward-facing state contains a considerably larger population of immobilized water molecules and displays conformational flexibility greater than that of the outward-facing state. Therefore, the entropy increase observed upon binding of Nb to WT LacY is likely due to release of bound water molecules mainly from the cytoplasmic

DOI: 10.1021/acs.biochem.6b00826
Biochemistry XXXX, XXX, XXX–XXX

cavity upon closure rather than an increase in protein conformational dynamics.

EXPERIMENTAL PROCEDURES

Reagents. Nitrophenyl α-galactoside (α-NPG) and nitrophenyl α-glucoside were purchased from Sigma-Aldrich, and undecyl β-D-maltopyranoside (UDM) was from Anatrace.

Plasmids and Strains. Construction of plasmids pT7-5/LacY[3] and pT7-5/G46W/G262W LacY,[7] each with a His tag at the C-terminus to allow metal affinity purification, has been described. T7-based expression plasmid p7XNH3/IIA^{Glc}-NH10 encoding *E. coli* IIA^{Glc} with a 10-His tag and a 9-residue linker at the N-terminus were constructed as described previously.[19] Overexpression of IIA^{Glc} or LacY was performed in the *E. coli* T7 Express strain (NEB) or XL1 Blue, respectively.

Nb Expression and Purification. Nb-9036 and Nb-9065 were expressed and purified as described previously.[29] Briefly, the cells were grown in LB broth with 2% glucose, 1 mM $MgCl_2$, and 100 mg/L ampicillin at 37 °C. Overnight cultures were inoculated [1:100 (v/v)] into Terrific Broth containing 0.1% glucose, 2 mM $MgCl_2$, and 100 mg/L ampicillin and shaken at 37 °C; 1 mM IPTG was added when A_{600} equaled 0.7, and cells were then shaken at 28 °C overnight. Cells were harvested by centrifugation, and the secreted Nb-9036 or Nb-9065 in the periplasm was obtained by osmotic shock and purified using cobalt-NTA affinity chromatography. Buffer exchange was performed to match the LacY solution by dialysis.

IIA^{Glc} Expression and Purification. Expression and purification of IIA^{Glc} were performed as described previously.[19] IIA^{Glc} in 20 mM Tris-HCl (pH 7.5), 100 mM NaCl, and 10% glycerol was purified by cobalt affinity chromatography and concentrated to approximately 100 mg/mL. Purified IIA^{Glc} is unphosphorylated.[19] UDM was added to match the LacY solution prior to ITC measurements.

LacY Expression and Purification. Cell growth and protein purification of LacY were conducted as described previously.[3,18] The purified protein was dialyzed with 20 mM Tris-HCl (pH 7.5), 100 mM NaCl, 0.035% UDM, and 10% glycerol at 20 mg/mL, flash-frozen in liquid nitrogen, and stored at −80 °C.

Protein Assay. The Micro BCA Protein Assay (Pierce Biotechnology, Inc.) was used for the protein concentration measurement.

Blue Native-PAGE. Blue native-12% PAGE[30] was conducted at 150 V for 3 h at 4 °C. All samples were supplemented with 0.12% UDM.

ITC. ITC measurements were performed in a Nano Isothermal Titration Calorimeter (TA Instruments). LacY in complex with Nb or IIA^{Glc} was placed in the sample cell with a reaction volume of 163 μL. The titrant (Nb, IIA^{Glc}, or α-NPG) was prepared in a buffer similar to the titrand in the sample cell, and 2 μL aliquots were injected incrementally into the sample cell at an interval of 300 s with constant stirring at 250 rpm. For binding of sugar to LacY or the LacY:Nb complex, α-NPGs were dissolved in dimethyl sulfoxide (DMSO) and diluted with assay buffer to 1 mM containing 0.5% DMSO. DMSO was added to the protein samples so that the buffers matched. Titration of nitrophenyl α-glucoside under identical conditions was used as a control.

ITC data processing was performed as described previously.[18] A correction for the heat of dilution was applied for a baseline-corrected thermogram by subtracting the integrated peak area from a constant estimated from the convergence value of the final injections. The corrected heat change (ΔQ) was plotted against the molar ratio of titrant versus titrand. The binding stoichiometry (N), association constant (K_a), and enthalpy change (ΔH) were directly determined by fitting the data using the one-site independent binding model provided by NanoAnalyze version 2.3.6. $K_d = 1/K_a$; $\Delta G = -RT \ln K_a$, where R is the gas constant (8.315 J K^{-1} mol^{-1}) and T is the absolute temperature. ΔS values were obtained by calculation using the equation $T\Delta S = \Delta H - \Delta G$.

Statistics. An unpaired t-test is used for data analysis. When $P > 0.1$, the difference is considered to be not statistically significant (ns). When $P = 0.05-0.1$, the difference is considered to be not quite statistically significant (±). When $P = 0.01-0.05$, the difference is considered to be statistically significant (*). When $P = 0.001-0.01$, the difference is considered to be very statistically significant (**).

Building the Model Systems. A simulation of the inward-facing crystal structure of LacY (PDB entry 2V8N), inserted into POPE lipids as published,[31] was extended from 85 to 210 ns. The outward-facing crystal structure (PDB entry 4ZYR) from the double-Trp mutant LacY was mutated back to the wild type, and the missing loop (residues 191−206) was built using Modeler.[32] The ligand α-NPG parameters were determined using MATCH[33] as described previously.[34] The protein model was inserted by aligning the protein center of mass with a POPE lipid bilayer containing 490 lipids generated by the CHARMM-GUI membrane builder.[35] The system was subsequently solvated by 18433 water molecules, and 59 Na^+ and 67 Cl^- ions were added to achieve electric neutrality and a salt concentration of 150 mM. The simulation system was relaxed using a 10000-step conjugate-gradient energy minimization followed by gradual heating, from 0 to 310 K over 120 ps. The lipids followed by the water molecules were then allowed to adjust to the restrained protein structure during consecutive 5 ns equilibration steps.

Simulation. The MD simulation was run with the NAMD 2.9 software package.[36] CHARMM22, including CMAP correction, and CHARMM36 force fields[37,38] were used for protein and lipids, respectively, and the TIP3P model was used for the water molecules.[39] A time step of 1 fs was used to integrate the equations of motion, and a reversible multiple-time step algorithm[40] of 4 fs was used for the electrostatic forces and 2 fs for short-range, nonbonded forces. The smooth particle mesh Ewald method[41,42] was used to calculate electrostatic interactions. The short-range interactions were cut off at 12 Å. All bond lengths involving hydrogen atoms were held fixed using the SHAKE[43] and SETTLE[44] algorithms. A Langevin dynamics scheme was used for thermostating, and Nosé−Hoover−Langevin pistons were used for pressure control.[45,46] Molecular graphics and simulation analyses were generated with VMD version 1.9.1.[47]

RESULTS

Nb Binding to Double-Trp LacY. Titration of the double-Trp mutant with Nb by ITC in the absence (black) or presence (gray) of melibiose yields exothermic titration thermograms (Figure 1c,i). The heat changes are due specifically to binding of Nb to the mutant because consecutive injection of Nb into the assay buffers without protein yields flat thermograms (Figure 1c,i, inset). The accumulated heat change (ΔQ on the right side) as a function of the molar ratio of Nb to LacY fits a one-site independent binding model (Figure 1d,j), yielding a binding stoichiometry near unity.

DOI: 10.1021/acs.biochem.6b00826
Biochemistry XXXX, XXX, XXX−XXX

Table 1. Nb Binding Assessed by ITC at 25 °C[a]

Titrant (Syringe)	Titrand (Cell)	Mel (mM)	K_d (nM)	ΔG [$\Delta\Delta G$][b]	ΔH [$\Delta\Delta H$]	$-T\Delta S$ [$-T\Delta\Delta S$]	N
				(kJ/mol)			
Nb-9036	Double-Trp mutant	0	59.8 (5.1[c])	-41.2 (0.2)	-49.4 (0.3)	8.2 (0.5)	1.0 (0.1)
		10	61.2 (8.4)	-41.2 (0.3)	-58.1 (2.6)	16.5 (2.1)	1.0 (0.1)
				[-0.0[ns]]	[-8.7[±]]	[8.3[±]]	
	WT LacY	0	114.4 (6.2)	-39.6 (0.2)	-20.1 (1.0)	-19.5 (1.1)	0.9 (0.1)
		10	39.3 (8.2)	-42.3 (0.5)	-38.1 (0.6)	-4.2 (0.7)	1.0 (0.1)
				[-2.7[*]]	[-18.0[**]]	[15.3[**]]	
Nb-9065	Double-Trp mutant	0	150.4 (15.4)	-39.0 (0.3)	-40.7 (0.2)	1.8 (0.0)	1.1 (0.0)
		10	340.7 (45.4)	-36.9 (0.3)	-42.9 (1.3)	5.9 (1.0)	1.0 (0.0)
				[2.1[*]]	[-2.2[ns]]	[4.1[±]]	
	WT LacY	0	896.5 (173.6)	-34.8 (0.5)	-12.6 (1.2)	-22.3 (1.5)	1.0 (0.1)
		10	138.6 (23.1)	-39.2 (0.5)	-31.4 (0.8)	-7.9 (1.3)	1.2 (0.1)
				[-4.4[*]]	[-18.9[**]]	[14.5[*]]	

[a]Data are from Figure 1. [b]Difference in the absence and presence of melibiose. [c]Standard error of the mean; two to five tests; *N*, stoichiometry. [ns]Not statistically significant. [±]Not quite statistically significant. [*]Statistically significant. [**]Very statistically significant.

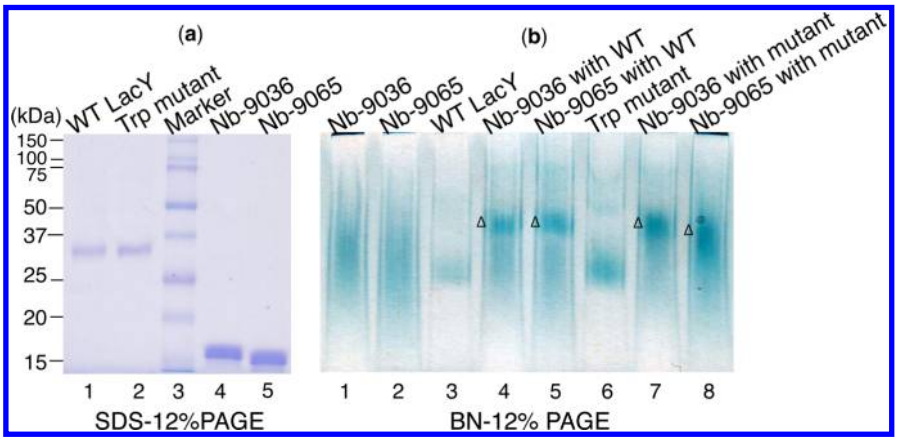

Figure 2. Formation of the Nb:LacY complex. (a) SDS−12% PAGE. WT LacY or the double-Trp mutant (~1 μg) was loaded in lane 1 or 2, respectively, without heating. Given Nbs (3 μg) were loaded in lane 4 or 5 after being heated at 95 °C for 15 min in the presence of 5 mM DTT. Molecular weight markers are given in lane 3. (b) Blue native-12% PAGE. Nbs (8 μg), WT LacY (4 μg), or the double-Trp mutant (4 μg) was loaded in the indicated lanes. WT LacY or the double-Trp mutant was mixed with a given Nb at a ratio of 1:2 prior to the analysis. Δ indicates the position of the Nb:LacY complexes.

Binding of Nb-9036 in the absence of melibiose exhibits a dissociation constant (K_d) of 59.8 ± 5.1 nM (Table 1), which is driven by a favorable enthalpy (ΔH, −49.4 ± 0.3 kJ/mol) with an entropy penalty ($-T\Delta S$, 8.2 ± 0.5 kJ/mol). The presence of melibiose does not affect binding affinity, but binding is slightly more enthalpic with more entropy compensation (Figure 1e). With Nb-9065, the K_d is 2- or 5-fold higher than that observed with Nb-9036 in the absence or presence of melibiose, respectively, and is also driven by enthalpy at an entropic cost (Figure 1k).

Nb Binding to WT LacY. Titration of WT LacY with Nb-9036 or -9065 (Figure 1f−h,l−n) causes a small release of heat (black), which is significantly increased by melibiose binding (gray). The K_d for Nb-9036 binding is 114.4 ± 6.2 nM, which is decreased by one-half to one-third in the presence of melibiose (Table 1). The K_d for Nb-9065 binding is 896.5 ± 173.6 nM, which is decreased by melibiose binding to approximately that of the mutant. Interestingly, binding of both Nbs to the WT in the absence or presence of melibiose is driven by both enthalpy and entropy (Figure 1h,n), which is different from binding with the mutant, in particular for Nb-9065, where increased entropy constitutes the main driving force in the absence of sugar. Melibiose binding significantly decreases the entropic contribution from 49 to 10% with Nb-9036 and from 64 to 20% with Nb-9065 (Table 1).

To illustrate complex formation directly, SDS−PAGE and Blue native-PAGE (BN-PAGE) were used to analyze formation of the protein complexes. Via SDS−PAGE, both the WT and the mutant (46.5 kDa) migrate with an M_r of ~35 kDa (lanes 1 and 2). Nb-9036 (~14.9 kDa) and Nb-9065 (~15.1 kDa) migrate with an M_r of around 15 kDa (Figure 2a). Via BN-PAGE (Figure 2b), the Nbs migrate as diffuse bands (lanes 1 and 2); the WT and the double-Trp mutant migrate as relatively focused bands (lanes 3 and 6). Both permeases shift to higher M_r values when they are premixed with either Nb (lanes 4, 5, 7, and 8), demonstrating that both proteins form stable complexes with either Nb.

Effect of Nb on Galactoside Affinity. Binding of α-NPG to LacY has been assessed by ITC.[17,18] The WT or the double-Trp mutant binds α-NPG with a K_d of 28.8 ± 2.1 or 5.0 ± 0.5 μM, respectively (Figure 3 and Table 2), each value similar to those obtained by other methods,[3,17,18,48−50] and titration with nitrophenyl α-D-glucopyranoside yields a small, relatively flat thermogram (Figure 3a, magenta). Energetically, α-NPG binding is favored by both enthalpy and entropy with the WT and by enthalpy at an entropic cost with the mutant. As

DOI: 10.1021/acs.biochem.6b00826
Biochemistry XXXX, XXX, XXX−XXX

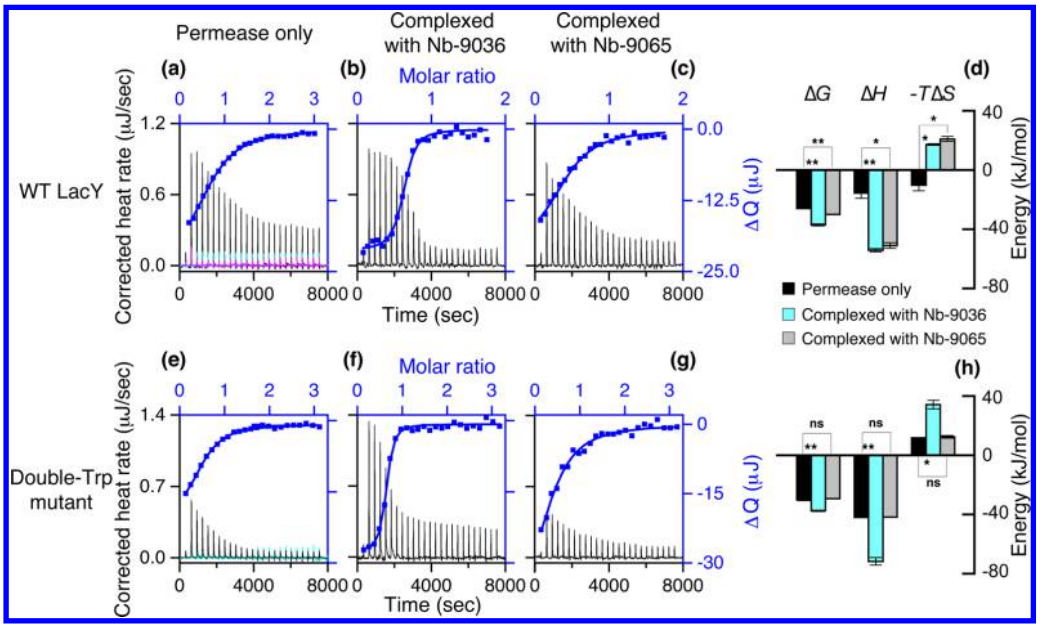

Figure 3. α-NPG binding in the absence or presence of a bound Nb. α-NPG at 1 or 0.2 mM was injected into the sample cell containing WT LacY (100 μM) or the G46W/G262W mutant (28 μM), respectively (a and e). WT LacY or the mutant preincubated with Nb-9036 (b and f) or Nb-9065 (c and g) at a ratio of 1:1.75 or 1:2.5, respectively, was titrated with α-NPG (0.2 mM). DMSO (0.5%) was present in both titrand and titrant for α-NPG solubility. Thermograms (a–c and e–g) were recorded at 25 °C. Injection of α-NPG into buffer at a concentration used for the titration into the protein samples is colored cyan (a and e), and injection of 1 mM nitrophenyl α-glucoside into the WT LacY is colored magenta (a). ΔQ (on the right side) vs α-NPG:LacY molar ratio (on the top) was fitted to a one-site independent binding model (blue curves), and the results are presented in Table 2 and panels d and f. (d and h) Comparison of α-NPG binding energies in the absence (black) and presence of Nb-9036 (cyan) or Nb-9065 (gray). An unpaired t-test was applied for the statastic anlaysis as described in the legand of Figure 1.

Table 2. Effects of Nb on the Affinity of WT LacY for α-NPG[a]

Titrant (Syringe)	Titrand (Sample Cell)	K_d (μM)	ΔG [$\Delta\Delta G$][b]	ΔH [$\Delta\Delta H$]	$-T\Delta S$ [$-T\Delta\Delta S$]	N
			(kJ/mol)			
α-NPG	WT LacY	28.8 (2.1[c])	-25.9 (0.2)	-15.6 (3.4)	-10.3 (3.6)	0.6 (0.1)
	WT:Nb-9036	0.3 (0.1)	-37.1 (0.6) [-11.2**]	-54.3 (1.1) [-38.7**]	17.2 (0.5) [27.5*]	0.5 (0.1)
	WT:Nb-9065	5.7 (0.1)	-30.0 (0.1) [-4.1**]	-51.0 (1.8) [-35.4*]	21.0 (1.7) [31.3*]	0.5 (0.0)
	Double-Trp mutant	5.0 (0.5)	-30.3 (0.3)	-42.1 (0.0)	11.8 (0.3)	0.5 (0.0)
	Mutant:Nb-9036	0.3 (0.0)	-37.5 (0.4) [-7.2**]	-71.7 (2.5) [-29.6**]	34.2 (2.9) [22.4*]	0.6 (0.0)
	Mutant:Nb-9065	7.1 (0.6)	-29.4 (0.2) [0.9ns]	-41.8 (1.05) [0.3ns]	12.43 (0.9) [0.6ns]	0.4 (0.0)

[a]Data are from Figure 3. [b]Difference in the absence and presence of Nb. [c]Standard error of the mean; two tests; N, stoichiometry. [ns]Not statistically significant. [*]Statistically significant. [**]Very statistically significant.

shown previously,[17,18] the stoichiometry of α-NPG binding determined by ITC does not approach unity for unknown reasons, but crystal structures[7,8] and biochemical studies[49,50] exhibit only a single galactoside-binding site. While this may alter absolute values of the thermodynamic parameters, the effects of Nb on energy changes provide useful information.

When a preincubated complex of Nb-9036 with WT or the mutant is titrated with α-NPG (Figure 3), a K_d of ~0.3 μM with both permease complexes is obtained, an approximate 96- or 19-fold decrease (i.e., increase in affinity), respectively (Table 2). Interestingly, titration of either the Nb-9065:WT or the Nb-9065:mutant complex with α-NPG yields a K_d similar to that of the mutant alone (i.e., a 4-fold decrease with the WT and no detectable change with the mutant). Thermodynamically, α-NPG binding with the complexes, except for the mutant complexed with Nb-9065, is driven by greater enthalpy ($\Delta\Delta H$ in a range of −29.6 to −38.7 kJ/mol) at a higher entropic cost ($-T\Delta\Delta S$ in the range of 22.4–31.3 kJ/mol) (Table 2 and Figure 3d). With α-NPG binding to the mutant complexed with Nb-9065, $\Delta\Delta G$, $\Delta\Delta H$, and $T\Delta\Delta S$ values are very small (Figure 1h), reflecting the lack of an effect of Nb-9065 on binding of α-NPG.[15]

Interplay of Binding of Nb and IIA^{Glc} to LacY. A previous study[18] showed that IIA^{Glc} does not bind to the double-Trp mutant, but binding to the cytoplasmic face of the WT is endothermic. To determine whether WT LacY can interact simultaneously with IIA^{Glc} and an Nb, the WT pre-equilibrated with Nb-9036 or -9065 in the presence of 10 mM melibiose was titrated with IIA^{Glc}, which exhibits flat exothermic thermograms (Figure 4) indicating no IIA^{Glc} binding.

DOI: 10.1021/acs.biochem.6b00826
Biochemistry XXXX, XXX, XXX–XXX

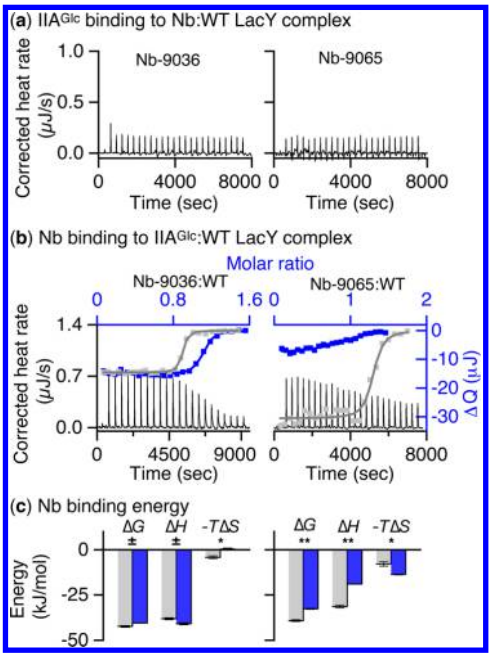

Figure 4. Interplay of binding of Nb and IIA^{Glc} to LacY at 25 °C. (a) IIA^{Glc} titration thermogram. Nb-9036 or Nb-9065 (66 μM) was premixed with LacY (40 μM) in the presence of 10 mM melibiose, and the complex was titrated with IIA^{Glc} (455 μM). (b) Binding of Nb to the LacY:IIA^{Glc} complex. LacY (40 μM) preincubated with IIA^{Glc} at a ratio of 1:2 was titrated with Nb-9036 (left) or Nb-9065 (right) at 170 μM in the presence of 10 mM melibiose. ΔQ values (right axis) were plotted vs Nb:LacY molar ratio (top axis) and fitted to a one-site independent binding model (blue color). The fitting data from binding of Nb to LacY without IIA^{Glc} (gray) were from Figure 1. (c) Histogram. Comparison of Nb binding energy in the absence (gray) and presence (blue) of IIA^{Glc}. Numerical values are listed in Table 3. An unpaired *t*-test was applied for the statastic anlaysis as described in the legand of Figure 1.

Titration of the IIA^{Glc}:WT LacY complex with Nb-9036 in the presence of melibiose shows that IIA^{Glc} has little effect on Nb binding (Table 3). However, IIA^{Glc} inhibits the binding affinity for Nb-9065 by 13-fold, as the result of a large decrease in enthalpy (Figure 4c). The data clearly suggest that Nb-9036 and Nb-9065 bind to different epitopes in LacY.

Water Dynamics in Internal Cavities of LacY. To identify the major contributors to the increase in entropy during binding of the ligand to WT LacY, the dynamics of water molecules and LacY in the two principal inward- and outward-facing states were analyzed by molecular dynamics (MD) simulations (Figure 5). The simulations were not designed to measure entropy quantitatively but rather to determine a qualitative molecular explanation for the quantitative experiments. To simulate the outward-facing state, the crystal structure of the double-Trp mutant with an occluded α-NPG molecule (PDB entry 4ZYR)[8] was "mutated" back to the WT. The simulation of the outward-facing state resulted in a periplasmic cavity slightly larger than that observed in the crystal structure (Figures 1b and 5b and Figure S1). It may not represent a completely realistic structural state because of limited temporal sampling. The previous simulation for an inward-facing state,[31] which is based on the inward-facing crystal structure of WT apo LacY (PDB entry 2V8N),[3] was extended to >200 ns. The simulated inward-facing state exhibits a smaller cytoplasmic cavity as described previously.[31]

The water-filled cytoplasmic or periplasmic cavities are divided into a central inner cavity with dimensions of 15 Å × 15 Å × 6 Å and an outer region termed the cytoplasmic or periplasmic gate region, respectively (Figure 5, top panels). The inner central cavities of both states are composed of the same residues. In the simulated inward- or outward-facing state, the number of water molecules in the central cavity is approximately 31 ± 3 or 21 ± 7, respectively (blue line, Figure 5a,b, middle panels). There are fewer water molecules in the simulated outward-facing state probably because of the presence of α-NPG. These results indicate that the number of water molecules in the common inner cavity remains relatively constant.

To characterize the water dynamics associated with the gate regions, the number of water molecules and residence times during the final 10 ns of each simulation were calculated (Figure 5, bottom panels). In the outward-facing state, the hydration dynamics in the periplasmic gate region is dominated by a large body of water molecules exhibiting shorter residence times, which indicates an efficient exchange between the protein cavity and the surrounding bulk water. In contrast, the water molecules associated with the cytoplasmic gate region in the simulated cytoplasmic-facing state show residence times significantly longer than that in the periplasmic gate region, implying a greater number of water molecules with reduced entropy.

The protein motions are analyzed by rmsd calculations for each trajectory with respect to the first simulation frame of the final 10 ns of each simulation. The simulated inward-facing

Table 3. Interplay of IIA^{Glc} and Nb with the LacY:Melibiose Binary Complex[a]

Titrant (Syringe)	Titrand (Sample Cell)	K_d (nM)	ΔG [$\Delta\Delta G$][b] (kJ/mol)	ΔH [$\Delta\Delta H$] (kJ/mol)	$-T\Delta S$ [$-T\Delta\Delta S$] (kJ/mol)	N
IIA^{Glc}	WT LacY:Nb-9036	ND	ND	ND	ND	
IIA^{Glc}	WT LacY:Nb-9065	ND	ND	ND	ND	
Nb-9036	WT LacY	39.3 (8.2)	-42.3 (0.5)	-38.1 (0.6)	-4.2 (0.7)	1.0 (0.1)
	WT LacY: IIA^{Glc}	80.5 (1.7)	-40.5 (0.1)	-40.9 (0.5)	0.4 (0.6)	1.0 (0.1)
			[1.8$^{\pm}$]	[-2.8$^{\pm}$]	[3.8*]	
Nb-9065	WT LacY	138.6 (23.1)	-39.2 (0.5)	-31.4 (0.8)	-7.9 (1.3)	1.2 (0.1)
	WT LacY: IIA^{Glc}	1,915.2 (255.2)	-32.7 (0.3)	-19.0 (0.2)	-13.7 (0.2)	0.9 (0.0)
			[6.5**]	[12.3**]	[-5.9*]	

[a]ITC was performed at 25 °C in the presence of 10 mM melibiose, and data are presented in Figure 4. [b]Difference in the absence and presence of IIA^{Glc}. [c]Standard error of the mean; two or three tests; *N*, stoichiometry; ND, not determined due to no binding. $^{\pm}$Not quite statistically significant. *Statistically significant. **Very statistically significant.

DOI: 10.1021/acs.biochem.6b00826
Biochemistry XXXX, XXX, XXX−XXX

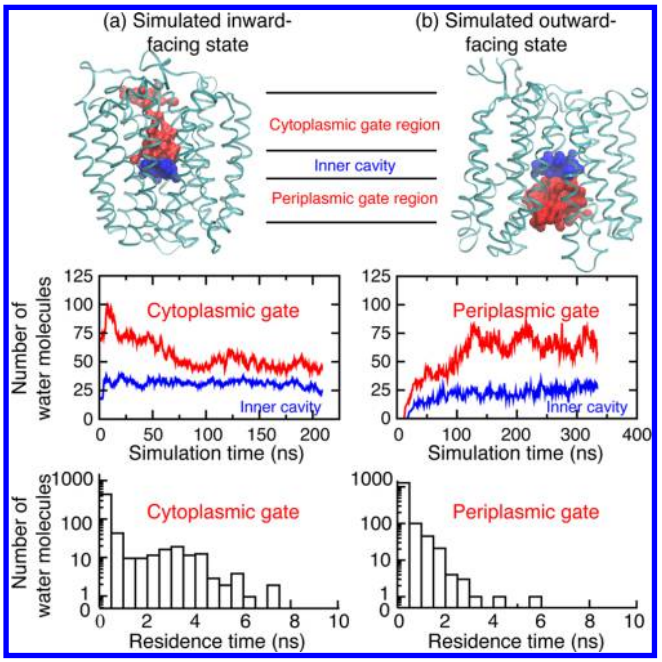

Figure 5. Water dynamics in LacY internal cavities. (a) Inward-facing conformation of WT apo LacY. (b) Outward-facing conformation of WT LacY with bound α-NPG. The top panels show backbone structures of the simulated inward-facing conformation based on the crystal structure of WT (PDB entry 2N8V) and the simulated outward-facing conformation with an occluded α-NPG molecule (derived from PDB entry 4ZYR). Water molecules extracted at the end of each simulation are colored blue (inner cavity) and red (cytoplasmic or periplasmic gate regions). Middle panels show the number of water molecules in the inner cavities (blue) or the gate regions (red) plotted vs time. The bottom panels show residence times of water molecules associated with cytoplasmic (left) or periplasmic gate (right) regions, presented as histograms with a log plot on the y axis.

state shows somewhat more pronounced conformational flexibility compared to that in the simulated outward-facing state (Figure S2). Hence, the simulations predict the entropy increase associated with the Nb-induced conformational transition from inward- to outward-facing states to be caused by release of immobilized water rather than an increase in conformational flexibility. In addition, conformational flexibility may be further decreased by binding of the Nb.

DISCUSSION

Release of trapped water molecules from proteins into the bulk solvent causes an increase in entropy because the motion-restricted water molecules on protein surfaces have less freedom (i.e., entropy) than in the bulk water phase. Therefore, as demonstrated,[51] water molecules within the SecY translocon exhibit anomalous diffusion with highly retarded rotational dynamics. For ligand binding, a common interpretation of the increase in entropy is based on the hydrophobic effect at the binding interface (i.e., ordered water molecules are released as hydrophobic groups interact),[26−28] but water molecules released from a protein may also result from structural rearrangements, such as the closure of hydrophilic cavities, in addition to the release of bound water from a binding interface or other regions. This consideration is especially important for transport proteins like permeases in the major facilitator superfamily[25,52−55] represented by LacY. These proteins have relatively larger water-filled cavities, and the transport cycles very likely involve formation of occluded intermediates and reciprocal opening and closing of cytoplasmic and periplasmic gate regions (Figures 1 and 5). Previous findings regarding interaction of IIA^{Glc} with WT LacY or MelB suggest a correlation between the increase in solvation entropy and the global conformational changes required for IIA^{Glc} binding.[18] Binding of Nb to LacY provides further support for this interpretation.

The resting state of WT LacY in the absence of substrate is the inward-facing conformation, while the resting state of the double-Trp mutant favors the opposite outward-facing conformation[3,9] (Figure 6a,b, state A), and galactoside binding is believed to induce both permeases to assume an occluded

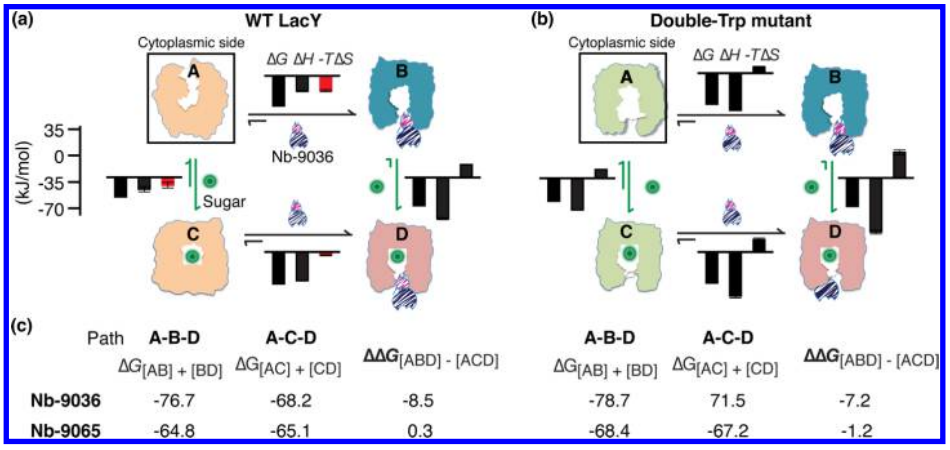

Figure 6. Thermodynamic cycle of Nbs and galactoside binding to WT or double-Trp LacY. (a) WT LacY and (b) double-Trp mutant. State A in panel a, cartoon of the simulated model of WT LacY based on the crystal structure (PDB entry 2V8N) that represents an inward-facing, lowest-free energy state.[3] State A in panel b, cartoon of the simulated double-Trp mutant model of the outward-facing state.[13,56] State B in panels a and b, proposed Nb-9036-bound outward-facing conformation.[15] State C in panels a and b, cartoons based on the crystal structure of the double-Trp mutant with an occluded galactoside (4OAA or 4ZYR).[7,8] State D in panels a and b, occluded intermediate for which k_{off} of galactoside is markedly inhibited.[15] Histograms are from Tables 1 and 2, and ΔG, ΔH, and $-T\Delta S$ are labeled with a scale at the right. (c) Thermodynamic cycle analysis. The conformational change from A to B to D is expressed as the A−B−D path, and that from A to C to D is expressed as the A−C−D path. The free energy difference between the two paths is expressed as $\Delta\Delta G_{[ABD]-[ACD]}$. The data for both Nb-9036 and -9065 are from Tables 1 and 2.

DOI: 10.1021/acs.biochem.6b00826
Biochemistry XXXX, XXX, XXX−XXX

intermediate conformation (Figure 6a,b, state C).[10] Stopped-flow measurements[15] of galactoside binding suggest that Nb-9036 stabilizes similar outward-facing conformations with either the WT or the double-Trp mutant (Figure 6a,b, state B) and that galactoside binding also induces a similar occluded intermediate with either the WT or the double-Trp mutant complexed with Nb-9036 (Figure 6a,b, state D).

While the binding affinity of Nb-9036 with either permease is similar, the entropy and enthalpy contributing to the binding free energy differ (Table 1 and Figure 6a,b, A → B, C → D). Binding to the outward-facing conformation of WT LacY (from an initial inward-facing state) is driven by both favorable enthalpy and entropy. In contrast, binding to the outward-facing conformation of the mutant (from an outward-facing conformation) is driven by a greater enthalpy with an entropic cost. Furthermore, when the WT is shifted into an occluded intermediate conformation by galactoside binding (state C), Nb-9036 binding is driven by a greater enthalpy ($\Delta\Delta H$ = −18.0 kJ/mol) at a higher cost of entropy ($-T\Delta\Delta S$ = 15.3 kJ/mol), indicating that galactoside binding promotes the binding of Nb-9036. With the double-Trp mutant that is already in an outward-facing conformation (Figure 6b, state A),[13] the effect of galactoside binding on enthalpy and entropy is smaller. In addition, direct measurements of galactoside binding (Table 2) with the inward-facing WT shows that formation of the fully liganded occluded state is driven by both favorable enthalpy and entropy. These binding energetics indicate that the increase in entropy correlates with the conformational change in WT LacY that closes the water-filled cytoplasmic gate region to form the occluded intermediate.

To identify the possible origins of the observed entropy increase, MD simulations of inward- and outward-facing conformations were performed. The water dynamics in the narrow, tunnel-like cytoplasmic gate region are significantly retarded (Figure 5a, bottom panel). It is conceivable that these immobilized water molecules will be released during the cytoplasmic closure and then gain entropy. This process is expected on a time scale of milliseconds, and it is out of reach for the current simulations. The simulated outward-facing state displays a periplasmic gate region that holds a large amount of water molecules with significantly shorter residence times, suggesting little difference between these cavity waters and bulk waters. Furthermore, while the Nb-bound structure is not available, rmsd calculations of the last 10 ns simulations suggest that the outward-facing state displays a lower degree of conformational dynamics compared to that in the inward-facing state. In addition, binding of Nb might reduce this conformational flexibility further. Thus, a greater entropic gain from water molecules released from LacY must compensate for the entropy loss due to hydration in the periplasmic gate region and for the loss in protein conformational dynamics. Because the cytoplasmic gate is the major region of the protein undergoing large structural changes that involve dehydration during the inward to outward transition, it is likely that the release of immobilized water from this cytoplasmic gate region is the primary factor contributing to the observed entropy increase associated with binding of Nb to WT LacY. It should be noted that a collective release or gain of water molecules in many places of LacY during the structural rearrangement as well as the LacY−Nb interactions may also contribute to the overall entropy increase to a lesser extent. Previously, a high solvation entropy for binding of IIA^{Glc} to WT LacY was detected.[18] These results are consistent with the previous notion that the larger number of bound water molecules released from LacY is primarily the result of closure of the cytoplasmic cavity.[18]

Binding of Nb-9065 to WT or the double-Trp mutant follows a trend similar to that of Nb-9036 binding. Galactoside binding causes insignificant changes in the enthalpy and entropy of Nb-9065 binding with the mutant but increases the affinity of WT for Nb-9065 to a level similar to that of the mutant, at a high cost of entropy ($-T\Delta\Delta S$ = 14.5 kJ/mol) (Table 1). The data further support the conclusion that the favorable entropy observed with the WT likely results from a large conformational change from the resting inward-facing state to the outward-facing state.

When WT LacY or the double-Trp mutant is complexed with Nb-9036, galactoside binding exhibits similar affinities, which resulted from a largely increased enthalpy ($\Delta\Delta H$ = −38.7 or −29.6 kJ/mol, respectively) at a higher entropic cost ($-T\Delta\Delta S$ = 27.5 or 22.4 kJ/mol, respectively) (Figure 6a,b), indicating positive coupling between galactoside binding and Nb-9036 binding. Nb-9065 also increases the galactoside affinity of WT LacY to a level similar to that of the double-Trp mutant (Table 2), which further supports the previous conclusion that both permeases probably assume similar conformations when Nb-9065 is bound, as is the case for Nb-9036[15] (Figure 6a,b, state B).

The energy contribution to move state A to state D can be further analyzed by comparing the total ΔG value from A−B−D path (Nb bound prior to sugar binding, state A to B to D) and A−C−D path (sugar bound prior to Nb binding, state A to C to D). With Nb-9065, the $\Delta G_{[ABD]}$ and $\Delta G_{[ACD]}$ values are similar within experimental error for either the WT or the mutant (Figure 6c), which conforms to a thermodynamic cycle. With Nb-9036, the $\Delta G_{[ABD]}$ value is significantly greater than $\Delta G_{[ACD]}$ [$\Delta\Delta G_{[ABD]-[ACD]}$ = −8.5 or −7.2 kJ/mol for the WT or mutant, respectively (Figure 6c)]. Thus, Nb-9036 interrupts the thermodynamic cycle by empowering LacY with a much greater galactoside binding affinity. Although the precise reason is unknown, Nb-9036 may provide extra contacts to the galactoside and/or generate a narrower diffusion pathway for bound sugar.

Taken together, these thermodynamic and molecular dynamics simulation studies suggest that the observed entropy increase coincident with binding of a ligand to LacY originates mainly from opposition of protein surfaces upon closure of the cytoplasmic cavity and release of immobilized water molecules.

■ ASSOCIATED CONTENT

Supporting Information

The Supporting Information is available free of charge on the ACS Publications website at DOI: 10.1021/acs.biochem.6b00826.

Superposition of the simulated model on the double-Trp crystal structure (Figure S1) and root-mean-square deviations (Figure S2) (PDF)

■ AUTHOR INFORMATION

Corresponding Authors

*E-mail: lan.guan@ttuhsc.edu.

*E-mail: rkaback@mednet.ucla.edu.

Funding

This work was supported by the National Science Foundation (Grant MCB-1158085 to L.G. and Eager Grant MCB-1547801

DOI: 10.1021/acs.biochem.6b00826
Biochemistry XXXX, XXX, XXX−XXX

to H.R.K.), the National Institutes of Health (Grant R01 GM095538 to L.G. and Grant R01 DK51131 to H.R.K.), a grant from Ruth and Bucky Stein (to H.R.K.), and a Marie Curie Career Integration Grant (FP7-MC-CIG-618558) and Åke Wibergs Stiftelse (M15-0148) to M.A. MD simulations were supported in part by the National Science Foundation through TeraGrid (now Xsede) resources provided by the Texas Advanced Computing Center at The University of Texas at Austin. We thank Instruct, part of the European Strategy Forum on Research Infrastructures (ESFRI), and the Hercules Foundation Flanders for their support.

Notes

The authors declare no competing financial interest.

■ ABBREVIATIONS

Nbs, nanobodies, recombinant variable fragments of camelid heavy chain antibodies (devoid of light chains); LacY, lactose permease of *E. coli*; MelB, melibiose permease; IIA^{Glc}, phosphotransferase protein of the glucose-specific phosphoenolpyruvate:carbohydrate phosphotransferase system; α-NPG, nitrophenyl α-galactoside; DMSO, dimethyl sulfoxide; BN-PAGE, Blue native-polyacrylamide gel electrophoresis; ITC, isothermal titration calorimetry; ΔH, enthalpy change; ΔS, entropy change; ΔG, free energy change; ΔQ, accumulated heat change; K_a, association constant; K_d, dissociation constant; MD, molecular dynamics; rmsd, root-mean-square deviation; PDB, Protein Data Bank; SDS−PAGE, sodium dodecyl sulfate−polyacrylamide gel electrophoresis; WT, wild-type.

■ REFERENCES

(1) Kaback, H. R., Sahin-Toth, M., and Weinglass, A. B. (2001) The kamikaze approach to membrane transport. *Nat. Rev. Mol. Cell Biol. 2*, 610−620.

(2) Guan, L., and Kaback, H. R. (2006) Lessons from lactose permease. *Annu. Rev. Biophys. Biomol. Struct. 35*, 67−91.

(3) Guan, L., Mirza, O., Verner, G., Iwata, S., and Kaback, H. R. (2007) Structural determination of wild-type lactose permease. *Proc. Natl. Acad. Sci. U. S. A. 104*, 15294−15298.

(4) Abramson, J., Smirnova, I., Kasho, V., Verner, G., Kaback, H. R., and Iwata, S. (2003) Structure and mechanism of the lactose permease of *Escherichia coli*. *Science 301*, 610−615.

(5) Chaptal, V., Kwon, S., Sawaya, M. R., Guan, L., Kaback, H. R., and Abramson, J. (2011) Crystal structure of lactose permease in complex with an affinity inactivator yields unique insight into sugar recognition. *Proc. Natl. Acad. Sci. U. S. A. 108*, 9361−9366.

(6) Mirza, O., Guan, L., Verner, G., Iwata, S., and Kaback, H. R. (2006) Structural evidence for induced fit and a mechanism for sugar/H(+) symport in LacY. *EMBO J. 25*, 1177−1183.

(7) Kumar, H., Kasho, V., Smirnova, I., Finer-Moore, J. S., Kaback, H. R., and Stroud, R. M. (2014) Structure of sugar-bound LacY. *Proc. Natl. Acad. Sci. U. S. A. 111*, 1784−1788.

(8) Kumar, H., Finer-Moore, J. S., Kaback, H. R., and Stroud, R. M. (2015) Structure of LacY with an alpha-substituted galactoside: Connecting the binding site to the protonation site. *Proc. Natl. Acad. Sci. U. S. A. 112*, 9004−9009.

(9) Smirnova, I., Kasho, V., and Kaback, H. R. (2011) Lactose permease and the alternating access mechanism. *Biochemistry 50*, 9684−9693.

(10) Kaback, H. R. (2015) A chemiosmotic mechanism of symport. *Proc. Natl. Acad. Sci. U. S. A. 112*, 1259−1264.

(11) Zhou, Y., Guan, L., Freites, J. A., and Kaback, H. R. (2008) Opening and closing of the periplasmic gate in lactose permease. *Proc. Natl. Acad. Sci. U. S. A. 105*, 3774−3778.

(12) Jiang, X., Nie, Y., and Kaback, H. R. (2011) Site-directed alkylation studies with LacY provide evidence for the alternating access model of transport. *Biochemistry 50*, 1634−1640.

(13) Smirnova, I., Kasho, V., Sugihara, J., and Kaback, H. R. (2013) Trp replacements for tightly interacting Gly-Gly pairs in LacY stabilize an outward-facing conformation. *Proc. Natl. Acad. Sci. U. S. A. 110*, 8876−8881.

(14) Kaback, H. R., Smirnova, I., Kasho, V., Nie, Y., and Zhou, Y. (2011) The alternating access transport mechanism in LacY. *J. Membr. Biol. 239*, 85−93.

(15) Smirnova, I., Kasho, V., Jiang, X., Pardon, E., Steyaert, J., and Kaback, H. R. (2014) Outward-facing conformers of LacY stabilized by nanobodies. *Proc. Natl. Acad. Sci. U. S. A. 111*, 18548−18553.

(16) Smirnova, I., Kasho, V., Jiang, X., Pardon, E., Steyaert, J., and Kaback, H. R. (2015) Transient conformers of LacY are trapped by nanobodies. *Proc. Natl. Acad. Sci. U. S. A. 112*, 13839−13844.

(17) Nie, Y., Smirnova, I., Kasho, V., and Kaback, H. R. (2006) Energetics of ligand-induced conformational flexibility in the lactose permease of *Escherichia coli*. *J. Biol. Chem. 281*, 35779−35784.

(18) Hariharan, P., Balasubramaniam, D., Peterkofsky, A., Kaback, H. R., and Guan, L. (2015) Thermodynamic mechanism for inhibition of lactose permease by the phosphotransferase protein IIA(Glc). *Proc. Natl. Acad. Sci. U. S. A. 112*, 2407−2412.

(19) Hariharan, P., and Guan, L. (2014) Insights into the inhibitory mechanisms of the regulatory protein IIA(Glc) on melibiose permease activity. *J. Biol. Chem. 289*, 33012−33019.

(20) Chao, Y., and Fu, D. (2004) Thermodynamic studies of the mechanism of metal binding to the *Escherichia coli zinc* transporter YiiP. *J. Biol. Chem. 279*, 17173−17180.

(21) Boudker, O., and Oh, S. (2015) Isothermal titration calorimetry of ion-coupled membrane transporters. *Methods 76*, 171−182.

(22) Pourcher, T., Leclercq, S., Brandolin, G., and Leblanc, G. (1995) Melibiose permease of *Escherichia coli*: large scale purification and evidence that H(+), Na(+), and Li(+) sugar symport is catalyzed by a single polypeptide. *Biochemistry 34*, 4412−4420.

(23) Maehrel, C., Cordat, E., Mus-Veteau, I., and Leblanc, G. (1998) Structural studies of the melibiose permease of *Escherichia coli* by fluorescence resonance energy transfer. I. Evidence for ion-induced conformational change. *J. Biol. Chem. 273*, 33192−33197.

(24) Guan, L., Nurva, S., and Ankeshwarapu, S. P. (2011) Mechanism of melibiose/cation symport of the melibiose permease of *Salmonella typhimurium*. *J. Biol. Chem. 286*, 6367−6374.

(25) Ethayathulla, A. S., Yousef, M. S., Amin, A., Leblanc, G., Kaback, H. R., and Guan, L. (2014) Structure-based mechanism for Na(+)/melibiose symport by MelB. *Nat. Commun. 5*, 3009.

(26) Dam, T. K., Torres, M., Brewer, C. F., and Casadevall, A. (2008) Isothermal titration calorimetry reveals differential binding thermodynamics of variable region-identical antibodies differing in constant region for a univalent ligand. *J. Biol. Chem. 283*, 31366−31370.

(27) Jelesarov, I., and Bosshard, H. R. (1994) Thermodynamics of ferredoxin binding to ferredoxin:NADP(+) reductase and the role of water at the complex interface. *Biochemistry 33*, 13321−13328.

(28) Olsson, T. S., Williams, M. A., Pitt, W. R., and Ladbury, J. E. (2008) The thermodynamics of protein-ligand interaction and solvation: insights for ligand design. *J. Mol. Biol. 384*, 1002−1017.

(29) Pardon, E., Laeremans, T., Triest, S., Rasmussen, S. G., Wohlkonig, A., Ruf, A., Muyldermans, S., Hol, W. G., Kobilka, B. K., and Steyaert, J. (2014) A general protocol for the generation of Nanobodies for structural biology. *Nat. Protoc. 9*, 674−693.

(30) Schagger, H., and von Jagow, G. (1991) Blue native electrophoresis for isolation of membrane protein complexes in enzymatically active form. *Anal. Biochem. 199*, 223−231.

(31) Andersson, M., Bondar, A. N., Freites, J. A., Tobias, D. J., Kaback, H. R., and White, S. H. (2012) Proton-coupled dynamics in lactose permease. *Structure 20*, 1893−1904.

(32) Sali, A., and Blundell, T. L. (1993) Comparative protein modelling by satisfaction of spatial restraints. *J. Mol. Biol. 234*, 779−815.

(33) Yesselman, J. D., Price, D. J., Knight, J. L., and Brooks, C. L., 3rd (2012) MATCH: an atom-typing toolset for molecular mechanics force fields. *J. Comput. Chem. 33*, 189−202.

DOI: 10.1021/acs.biochem.6b00826
Biochemistry XXXX, XXX, XXX−XXX

(34) Jiang, X., Villafuerte, M. K., Andersson, M., White, S. H., and Kaback, H. R. (2014) Galactoside-binding site in LacY. *Biochemistry 53*, 1536−1543.
(35) Jo, S., Kim, T., and Im, W. (2007) Automated builder and database of protein/membrane complexes for molecular dynamics simulations. *PLoS One 2*, e880.
(36) Phillips, J. C., Braun, R., Wang, W., Gumbart, J., Tajkhorshid, E., Villa, E., Chipot, C., Skeel, R. D., Kale, L., and Schulten, K. (2005) Scalable molecular dynamics with NAMD. *J. Comput. Chem. 26*, 1781−1802.
(37) Mackerell, A. D., Jr., Feig, M., and Brooks, C. L., 3rd (2004) Extending the treatment of backbone energetics in protein force fields: limitations of gas-phase quantum mechanics in reproducing protein conformational distributions in molecular dynamics simulations. *J. Comput. Chem. 25*, 1400−1415.
(38) Klauda, J. B., Venable, R. M., Freites, J. A., O'Connor, J. W., Tobias, D. J., Mondragon-Ramirez, C., Vorobyov, I., MacKerell, A. D., Jr., and Pastor, R. W. (2010) Update of the CHARMM all-atom additive force field for lipids: validation on six lipid types. *J. Phys. Chem. B 114*, 7830−7843.
(39) Jorgensen, W., Chandrasekhar, J., Madura, J., Impey, R., and Klein, M. (1983) Comparison of simple potential functions for simulating liquid water. *J. Chem. Phys. 79*, 926−935.
(40) Grubmüller, H., Heller, H., Windemuth, A., and Schulten, K. (1991) Generalized Verlet Algorithm for Efficient Molecular Dynamics Simulations with Long-range Interactions. *Mol. Simul. 6*, 121−142.
(41) Darden, T., York, D., and Pedersen, L. (1993) Particle mesh Ewald: An N·log(N) method for Ewald sums in large systems. *J. Chem. Phys. 98*, 10089−10092.
(42) Essmann, U., Perera, L., Berkowitz, M., Darden, T., Lee, H., and Pedersen, L. (1995) A smooth particle mesh Ewald method. *J. Chem. Phys. 103*, 8577−8593.
(43) Ryckaert, J.-P., Ciccotti, G., and Berendsen, H. (1977) Numerical integration of the cartesian equations of motion of a system with constraints: molecular dynamics of n-alkanes. *J. Comput. Phys. 23*, 327−341.
(44) Miyamoto, S., and Kollman, P. (1992) Settle: An analytical version of the SHAKE and RATTLE algorithm for rigid water models. *J. Comput. Chem. 13*, 952−962.
(45) Feller, S., Zhang, Y., Pastor, R., and Brooks, B. (1995) Constant pressure molecular dynamics simulation: The Langevin piston method. *J. Chem. Phys. 103*, 4613−4621.
(46) Martyna, G., Tobias, D., and Klein, M. (1994) Constant pressure molecular dynamics algorithms. *J. Chem. Phys. 101*, 4177−4189.
(47) Humphrey, W., Dalke, A., and Schulten, K. (1996) VMD: Visual molecular dynamics. *J. Mol. Graphics 14*, 33−38.
(48) Smirnova, I. N., Kasho, V., and Kaback, H. R. (2008) Protonation and sugar binding to LacY. *Proc. Natl. Acad. Sci. U. S. A. 105*, 8896−8901.
(49) Sahin-Toth, M., Lawrence, M. C., Nishio, T., and Kaback, H. R. (2001) The C-4 hydroxyl group of galactopyranosides is the major determinant for ligand recognition by the lactose permease of *Escherichia coli*. *Biochemistry 40*, 13015−13019.
(50) Guan, L., and Kaback, H. R. (2004) Binding affinity of lactose permease is not altered by the H+ electrochemical gradient. *Proc. Natl. Acad. Sci. U. S. A. 101*, 12148−12152.
(51) Capponi, S., Heyden, M., Bondar, A. N., Tobias, D. J., and White, S. H. (2015) Anomalous behavior of water inside the SecY translocon. *Proc. Natl. Acad. Sci. U. S. A. 112*, 9016−9021.
(52) Deng, D., Xu, C., Sun, P., Wu, J., Yan, C., Hu, M., and Yan, N. (2014) Crystal structure of the human glucose transporter GLUT1. *Nature 510*, 121−125.
(53) Quistgaard, E. M., Low, C., Moberg, P., Tresaugues, L., and Nordlund, P. (2013) Structural basis for substrate transport in the GLUT-homology family of monosaccharide transporters. *Nat. Struct. Mol. Biol. 20*, 766−768.
(54) Nomura, N., Verdon, G., Kang, H. J., Shimamura, T., Nomura, Y., Sonoda, Y., Hussien, S. A., Qureshi, A. A., Coincon, M., Sato, Y., Abe, H., Nakada-Nakura, Y., Hino, T., Arakawa, T., Kusano-Arai, O., Iwanari, H., Murata, T., Kobayashi, T., Hamakubo, T., Kasahara, M., Iwata, S., and Drew, D. (2015) Structure and mechanism of the mammalian fructose transporter GLUT5. *Nature 526*, 397−401.
(55) Pedersen, B. P., Kumar, H., Waight, A. B., Risenmay, A. J., Roe-Zurz, Z., Chau, B. H., Schlessinger, A., Bonomi, M., Harries, W., Sali, A., Johri, A. K., and Stroud, R. M. (2013) Crystal structure of a eukaryotic phosphate transporter. *Nature 496*, 533−536.
(56) Smirnova, I., Kasho, V., Sugihara, J., and Kaback, H. R. (2011) Opening the periplasmic cavity in lactose permease is the limiting step for sugar binding. *Proc. Natl. Acad. Sci. U. S. A. 108*, 15147−15151.

DOI: 10.1021/acs.biochem.6b00826
Biochemistry XXXX, XXX, XXX−XXX